Conversion of plasma VLDL and IDL precursors into various LDL subpopulations using density gradient ultracentrifugation

Carol A. Marzetta,[1] David M. Foster, and John D. Brunzell

Department of Medicine and Center for Bioengineering, University of Washington, Seattle, WA 98195

Abstract The contribution of very low density lipoproteins (VLDL) and intermediate density lipoproteins (IDL) to various low density lipoprotein (LDL) subfractions was examined in three normal subjects and two with familial combined hyperlipidemia. Autologous VLDL + IDL (d < 1.019 g/ml) or VLDL only (d < 1.006 g/ml; one subject only) were isolated by sequential ultracentrifugation, iodinated, and injected into each subject. The appearance, distribution, and subsequent disappearance of radioactivity into LDL density subpopulations was characterized using density gradient ultracentrifugation. These techniques help determine the contribution of precursors to various LDL subpopulations defined uniquely for each subject. The results from these studies have suggested: *1*) it took up to several days of intravascular processing of precursor-derived LDL before it resembled the distribution of the 'steady-state' plasma LDL protein; *2*) plasma VLDL and IDL precursors contributed rapidly to a broad density range of LDL; *3*) the radiolabeled plasma precursors did not always contribute to all LDL density subfractions within an individual in proportion to their relative LDL protein mass as determined by density gradient ultracentrifugation; *4*) with time, the distribution of the precursor-derived LDL became more buoyant or more dense than distribution of the LDL protein mass; and *5*) the kinetic characteristics of precursor-derived particles within LDL changed within a relatively narrow density range and were not always related to the LDL density heterogeneity of each subject. These studies emphasize the complexities of apoB metabolism and the need to design studies to carefully examine the production of various LDL subpopulations, the kinetic fate and interconversions among the subpopulations, and ultimately, their relationship to the development of atherosclerosis. —**Marzetta, C. A., D. M. Foster, and J. D. Brunzell.** Conversion of plasma VLDL and IDL precursors into various LDL subpopulations using density gradient ultracentrifugation. *J. Lipid Res.* 1990. **31:** 975–984.

Supplementary key words apoprotein B • very low density lipoprotein • low density lipoprotein

LDL have been characterized as a class of heterogeneous particles that differ in size, density, lipid and apoprotein composition, and metabolism (1–8). The fundamental pathway describing the production of LDL has traditionally been thought to involve the production of VLDL by the liver with the subsequent conversion of VLDL to IDL and then to LDL by a series of events involving the hydrolysis and removal of triglyceride from the core of the particles (9, 10). More recently, however, alternative pathways for production of LDL have been suggested which involve the direct production of LDL-like particles from the liver (11–15) and/or the rapid conversion of small nascent VLDL or IDL precursors pools to plasma LDL (16–18). While it has been suggested that up to 50% of plasma LDL can be derived from plasma VLDL-independent sources in normolipidemic subjects (17), it is unclear whether certain LDL subfractions are derived from specific plasma precursors such as VLDL and IDL while others are derived preferentially by direct production.

Although several studies have examined the contribution of plasma VLDL precursors to different density cuts of LDL (6, 7, 19), there is little information available on the relationships between plasma precursors and various plasma LDL subpopulations. The current studies were designed to examine the conversion of radiolabeled VLDL and IDL precursors into various LDL density subpopulations in three normolipidemic individuals and two subjects with familial combined hyperlipidemia. The distribution of precursor-derived radioactivity was followed with time among the LDL density subpopulations unique to each subject using density gradient ultracentrifugation.

Abbreviations: d, density in g/ml; DGUC, density gradient ultracentrifugation; EDTA, ethylenediaminetetraacetic acid; FCHL, familial combined hypercholesterolemia; fx, fraction; IDL, intermediate density lipoprotein; LDL-C, low density lipoprotein cholesterol; LTP, lipid transfer protein; SDS-PAGGE, sodium dodecyl sulfate-polyacrylamide gradient gel electrophoresis; TPC, total plasma cholesterol; VLDL-C, very low density lipoprotein cholesterol.

[1]Present address: Pfizer Central Research, Department of Metabolic Diseases, Eastern Point Road, Groton, CT 06340.

MATERIALS AND METHODS

Subjects

Five subjects, three normolipidemic subjects (JT, MC, DW; subjects 1, 2, and 3, respectively, of ref. 20) and two subjects with familial combined hyperlipidemia (FCHL) (subjects WE and HM; subjects 4, and 5, respectively, of ref. 20) were studied as outpatients of the Clinical Research Center at the University Hospital of the University of Washington after informed patient consent and approval by the Human Subjects Review Committee of the University of Washington. Detailed clinical parameters for each subject have been published elsewhere (20). Mean total plasma cholesterol, triglyceride, and apoB concentrations in the control and FCHL groups were 178 ± 50, 59 ± 15, 94 ± 31, and 270, 160, 142 mg/dl, respectively. The subjects with FCHL were diagnosed according to the criteria described previously (20). Subject HM was taking ethinyl estradiol (0.05 mg, qd). No other subject was receiving medication known to alter lipid metabolism. Each subject maintained his/her usual diet throughout the study. Potassium iodide (500 mg) was given orally three times a day beginning 3 days before the injection of radiolabeled lipoproteins and throughout the study.

Preparation of radiolabeled lipoproteins

A blood sample was taken from each subject after an overnight fast and placed immediately into tubes on ice containing 1 mg/ml EDTA, 1 mg/ml NaN_3, and 10 U aprotinin (final concentrations). Plasma was isolated by centrifugation at 2600 *g* for 30 min at 4°C. VLDL ($d < 1.006$ g/ml) or VLDL + IDL ($d < 1.019$ g/ml) and LDL ($1.019 < d < 1.063$ g/ml) were isolated from plasma by sequential ultracentrifugation using a 60 Ti rotor (20) Between 3.5 to 5.3 mg of lipoprotein protein was iodinated with ^{125}I or ^{131}I (New England Nuclear, Boston, MA) by the method of McFarlane (21) as modified by Bilheimer, Eisenberg, and Levy (22). Less than 3% of the radioactivity in the VLDL or VLDL + IDL preparations was free iodine. An average of 58.9 + 13% of the total radioactivity was isolated in apoB-100 as measured by SDS-PAGGE and 11.2 + 1.0% was lipid-extractable. The radiolabeled lipoproteins were sterilized using a 0.2-μm filter and checked for pyrogenicity before injection.

Design of the studies

Each subject was injected simultaneously with 50 μCi of ^{131}I-VLDL (subject WE) or ^{125}I-labeled VLDL + IDL (subjects JT, MC, DW, and HM) and 50 μCi of ^{125}I- or ^{131}I-labeled LDL after an overnight fast. The LDL turnover studies have been described in detail previously (20). Blood samples were obtained 10 min, 3, 6, 9, 24, 34, 48, and 58 h, and then daily (8 AM after an overnight fast) for up to 9 days after the injection of radiolabeled lipoproteins. Plasma was isolated from each blood sample as described earlier and aliquots were taken to determine total whole plasma radioactivity. Radioactivity was quantitated using a Packard 5160 gamma counter (Lahuna Hills, CA) and corrections were made for background, spillover, quench, and decay of each isotope.

Lipoprotein separation and characterization

The density distribution of the radiolabeled lipoproteins was determined using density gradient ultracentrifugation (DGUC; 20). Briefly, whole plasma was underlayered into a discontinuous salt gradient and subjected to ultracentrifugation in an SW-41 rotor at 41,000 rpm for 24 h at 15°C. For subject HM, VLDL ($d < 1.006$ g/ml) was first isolated from whole plasma by ultracentrifugation in a 40.3 rotor at 40,000 rpm for 18 h at 10°C and the $d > 1.006$ g/ml fraction was then subjected to DGUC as described. For each DGUC run, a tube containing the same density solutions but without the lipoprotein sample was prepared at the same time. After ultracentrifugation, each sample was drained and 38–43 fractions were collected as described previously (20) The refractive index (ABBE-3L Refractometer; Bausch and Lomb, Rochester, NY) was measured at 15°C on alternate fractions of the blank sample. The density for each fraction was determined using standard solutions of known densities and their refractive index. The distribution of radioactivity among the lipoprotein fractions was determined by counting each fraction and correcting for background, spillover, quench, and decay. The average percentage of recovery of radioactivity after DGUC for a representative study was 91.9 ± 6% (mean ± SD; n = 12). The LDL DGUC profiles that reflect relative LDL protein mass or absorbance at 280 nm are referred to as LDL protein mass for simplicity.

ApoB radioactivity determinations and chemical analyses

After DGUC, specific fractions were pooled based on the relative protein profiles of each subject (arbitrarily designated as VLDL, IDL, and LDL_1 and LDL_2). ApoB radioactivity was determined in each pooled subfraction (defined specifically for each subject throughout the text) by isopropanol precipitation (23) and SDS-polyacrylamide gradient gel electrophoresis (SDS-PAGGE) to check for apoB-48 contamination (24). For SDS-PAGGE, the bands corresponding to each apoprotein were sliced and counted. In all studies, less than 3% of the total radioactivity was isolated in the apoB-48 band. The plasma disappearance curves for each individual fraction within LDL_1 and LDL_2 were corrected for apoB radioactivity based on the percentage of radioactivity isolated in apoB within each pooled subpopulation.

Total plasma cholesterol and triglyceride and lipoprotein cholesterol concentrations were measured according

to the methods outlined by the Lipid Research Clinic (25). ApoB measurements on the pooled lipoprotein subpopulations (VLDL, IDL, LDL_1, and LDL_2) were determined using the RIA methods of Albers, Cabana, and Hazzard (26).

RESULTS

The disappearance of VLDL + IDL-derived apoB radioactivity and its appearance into the LDL density range (as defined by the DGUC profiles) for a representative normolipidemic subject (JT) and FCHL subject (HM) are shown in **Fig. 1**. In the normolipidemic subject JT, the maximum appearance of precursor-derived apoB radioactivity into LDL (21.2%) occurred approximately 24 h after injection of the radiolabled lipoproteins, whereas in FCHL subject HM, this peak occurred approximately 48 h after the injection of the radiolabeled lipoproteins and represented 18.0% of the injected apoB radioactivity. For all subjects, the maximal appearance of precursor-derived apoB radioactivity into the LDL density range varied between 10 and 48 h after the injection of the radiolabeled lipoproteins and was positively correlated to total plasma cholesterol (TPC) concentrations [$r = 0.85$; time of peak = 0.008(TPC) – 0.548; $P < 0.007$], plasma TG concentrations [$r = 0.99$; time of peak = 0.010 (TG) + 0.218; $P = 0.002$], plasma apoB concentrations [$r = 0.84$; time of peak = 0.014(apoB) – 0.427; $P = 0.07$], VLDL cholesterol (VLDL-C) concentrations [$r = 0.94$; time of peak = 0.088(VLDL-C) – 1.254; $P < 0.02$], and LDL cholesterol (LDL-C) concentrations [$r = 0.63$; time of peak = 0.006(LDL-C) + 0.269; $P = 0.26$].

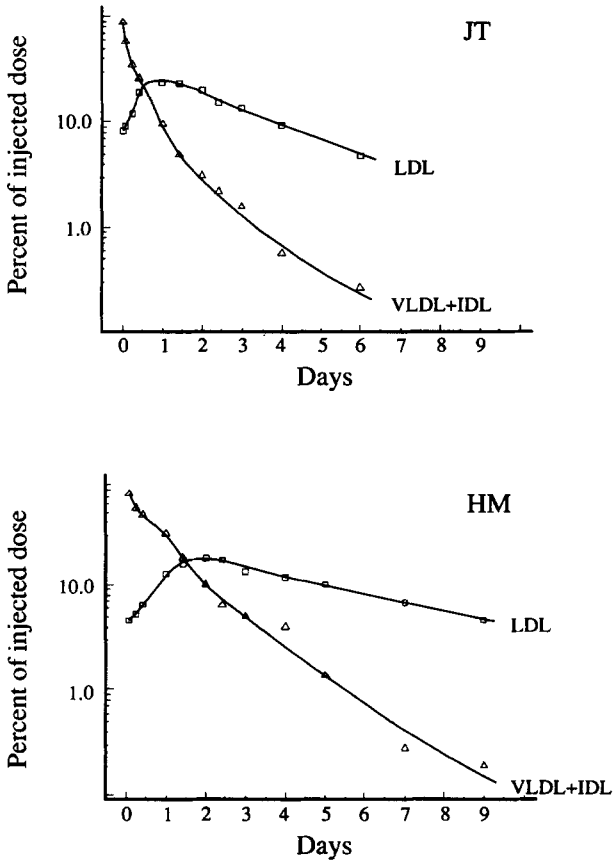

Fig. 1. Disappearance of radiolabeled VLDL + IDL apoB radioactivity from plasma and its appearance into LDL as defined by DGUC; △, VLDL + IDL; □, LDL. The symbols represent the observed data, the lines are drawn by hand. JT, normolipidemic; HM, FCHL.

Since each data point along the plasma disappearance and appearance curves actually represents the sum of the radioactivity distributed among all the lipoprotein subpopulations, the distribution of the precursor-derived apoB radioactivity among the various LDL products was examined in more detail using DGUC. For all subjects, the distribution of the radioactivity at the time in which the maximal appearance of precursor-derived apoB radioactivity was isolated within the LDL density range was never superimposable with the distribution of the LDL protein mass. As shown in normolipidemic subject JT, at 24 h (maximum LDL apoB radioactivity; see Fig. 1), the peak density of the radiolabeled lipoproteins distributed primarily in a more buoyant region (1.034 g/ml) compared to the plasma LDL protein mass (1.041 g/ml **Fig. 2**, 1 day). Similarly, in FCHL subject HM, at 48 h (maximum LDL apoB radioactivity; see Fig. 1) the peak density of the radiolabeled lipoproteins was 1.038 g/ml compared to the peak density of the LDL mass which was 1.042 g/ml (**Fig. 3**, 2 days).

With time, variable amounts of precursor-derived apoB radioactivity were isolated within the LDL density range defined uniquely by the DGUC profiles for each subject (12–38%; calculated as the maximum apoB radioactivity isolated within LDL_1 plus LDL_2 after separation by DGUC divided by the injected dose). With time, in the normolipidemic subjects the precursor-derived radioactivity distributed among the various LDL subpopulations and resembled the protein distribution of the plasma LDL. As shown for normolipidemic subject JT, 3 days after the injection of radiolabeled lipoproteins, the distribution of the radiolabled lipoproteins resembled the distribution of the plasma LDL protein mass (Fig. 2, 3 days). However, with time in this subject, the peak density of the radiolabeled lipoproteins became more dense (1.047 g/ml) compared to the density of the plasma LDL (1.0415 g/ml; Fig. 2, 6 days).

In contrast, in both FCHL subjects the distribution of the precursor-derived radioactivity never resembled the distribution of the protein mass. As illustrated in Fig. 3, with time the distribution of the precursor-derived radioactivity remained in a more buoyant region (1.039 g/ml) compared to the LDL protein mass (1.043 g/ml) even 7 days after the injection of the radiolabeled lipoproteins (Fig. 3, lower panel).

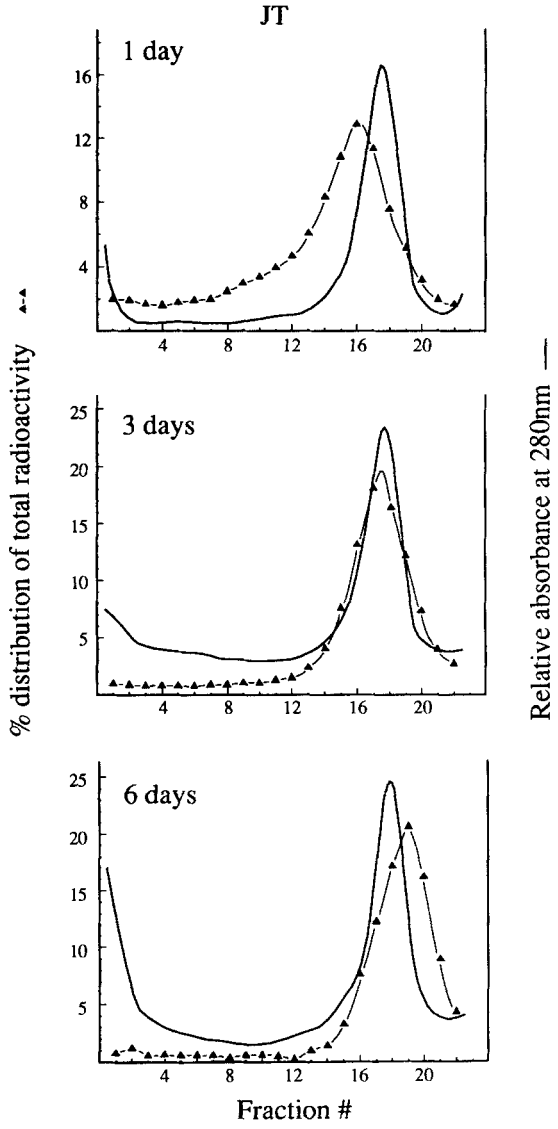

Fig. 2. Density gradient ultracentrifugation profiles of the distribution of relative protein mass (—) and VLDL + IDL-derived total radioactivity (▲) among apoB-containing lipoproteins isolated from normolipidemic subject JT 1, 3, and 6 days after the injection of radiolabeled lipoproteins.

To examine the metabolic behavior of various lipoproteins in more detail, fractions within specific density ranges (arbitrarily chosen and designated as VLDL, IDL, LDL_1, and LDL_2 based on the density gradient profiles unique to each subject) were pooled and apoB radioactivity was determined for each subpopulation as described previously. The disappearance of radiolabeled apoB from VLDL in normolipidemic subject JT (fractions 1–8 $d < 1.017$ g/ml; **Fig. 4**, upper panel), decreased rapidly within the first day and then disappeared at slower rate. A prominent delay in the disappearance of radioactivity was seen in the IDL subpopulation (fractions 9–13; $1.017 < d < 1.026$ g/ml). The appearance of precursor-derived radioactivity into LDL occurred rapidly in both the buoyant (fractions 14–16; $1.026 < d < 1.036$ g/ml) and dense (fractions 17–21; $1.036 < d < 1.060$ g/ml) LDL subpopulations. However, approximately 10 h after the injection of the radiolabeled lipoproteins, radioactivity within the LDL_1 subpopulation disappeared at a rate similar to that seen in the IDL subpopulation. In contrast, radioactivity within the LDL_2 subpopulation continued to increase until about 1.5 days and then disappeared at a much slower rate compared to LDL_1 (Fig. 4, JT).

In FCHL subject HM, the general metabolic characteristics of the VLDL and IDL subpopulations were similar to the normal subjects (Fig 4, lower panel). That

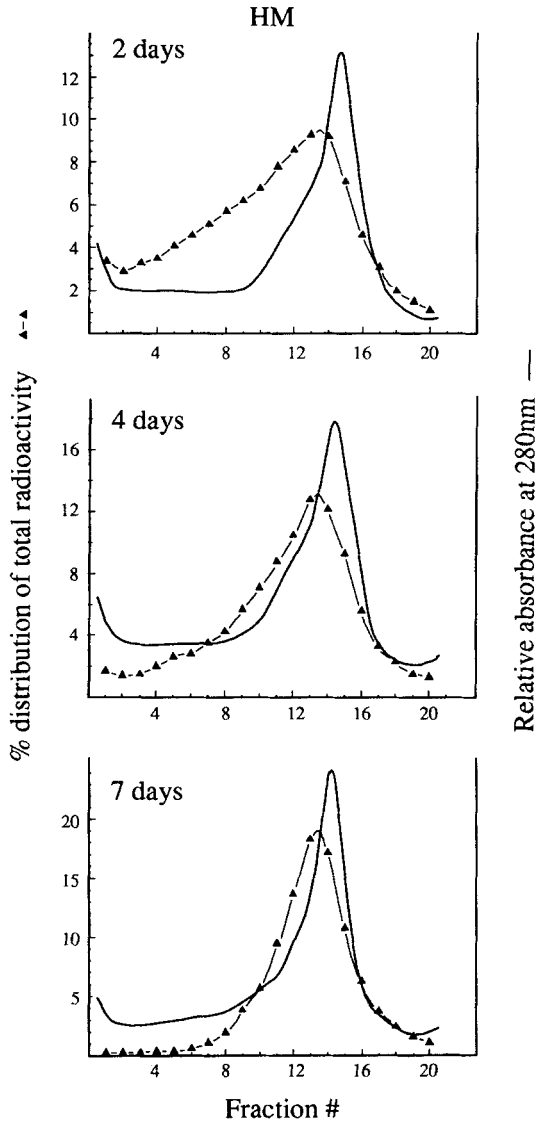

Fig. 3. Density gradient ultracentrifugation profiles of the distribution of relative protein mass (—) and VLDL + IDL-derived total radioactivity (▲) among apoB containing lipoproteins isolated from FCHL subject HM 2, 4, and 7 days after the injection of radiolabeled lipoproteins.

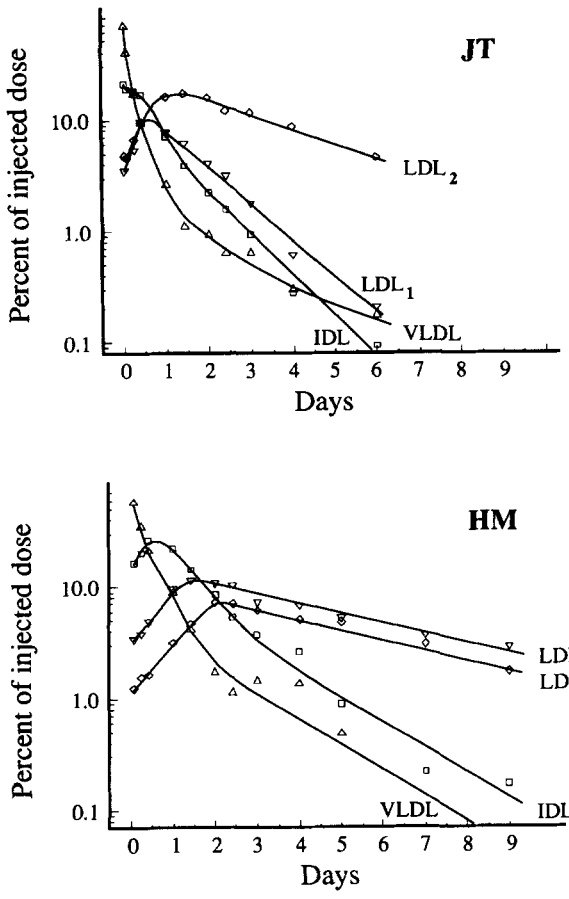

Fig. 4. The disappearance and appearance of apoB radioactivity from VLDL (△), IDL (□), LDL_1 (▽), and LDL_2 (◇) as defined by the DGUC profiles. The symbols represent the observed data and the lines are drawn by hand. JT, normolipidemic; HM, FCHL.

is, there was an initial rapid disappearance of radioactivity from VLDL ($d < 1.006$ g/ml) followed by a slower rate of disappearance and an initial increase of radioactivity into IDL (fractions 1-8; $d < 1.0275$ g/ml) followed by rapid and then slower disappearance from this subpopulation. As in the normolipidemic subject, the rate of appearance of precursor-derived radioactivity increased similarly into buoyant and dense LDL, however unlike JT, the rate of disappearance from LDL_1 (fractions 9-13; $1.0275 < d < 1.042$ g/ml) and LDL_2 (fractions 14-19; $1.042 < d < 1.069$ g/ml) after 2 days was nearly identical (Fig. 4, HM). Similar rates of disappearance in both LDL subpopulations were also seen in normolipidemic subjects MC and DW whereas the disappearance of radioactivity from LDL_1 and LDL_2 from FCHL subject WE was more similar to subject JT (data not shown).

Although dividing LDL into buoyant and dense subpopulations was based on the DGUC protein profiles unique to each individual, it was clear that the density heterogeneity in some of the subjects was more complex (see Fig. 1 of ref. 20). To obtain additional information on the relationships between the general kinetic characteristic and density heterogeneity of each subject's LDL subpopulations, the appearance and disappearance of radioactivity with time was examined in each fraction within LDL_1 and LDL_2 as defined by DGUC. Individual fractions within the buoyant and dense subpopulations have been corrected for apoB radioactivity determined for each pooled subpopulation as described earlier. Within the LDL_1 subpopulation in normolipidemic subject JT, the increase in radioactivity into fractions 14, 15, and 16 was similar and rapid; however, the peak of the radiolabel occurred first in the most buoyant fraction (fx 14), followed in order by fractions 15 and 16 (**Fig. 5**, LDL_1). Although the rate of removal after the initial increase of radioactivity into each fraction was relatively rapid, the final rate of disappearance slowed progressively with in-

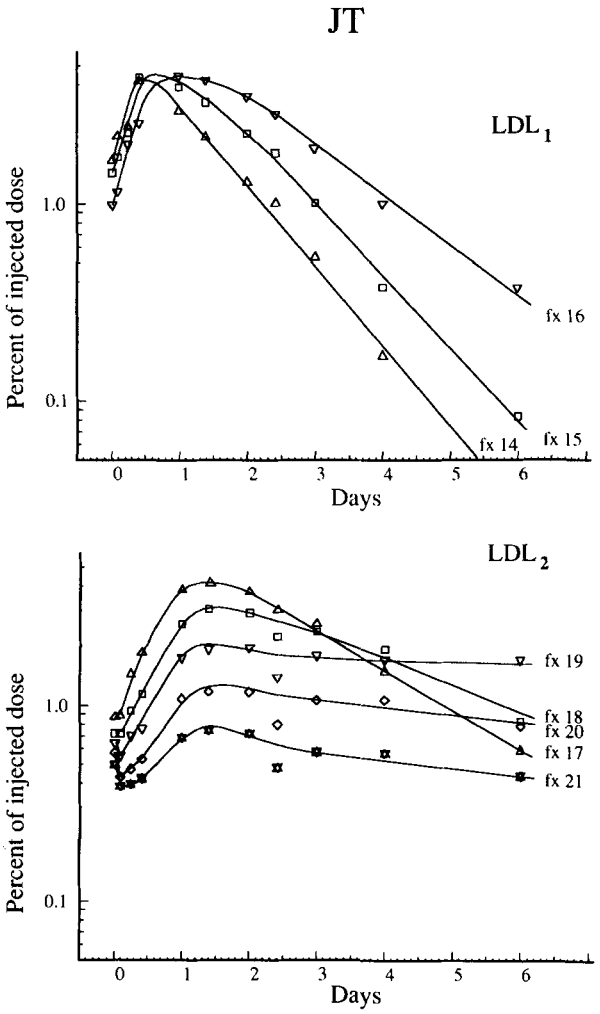

Fig. 5. The appearance and disappearance of VLDL + IDL-derived apoB radioactivity with time in each fraction isolated within the LDL density range after separation by DGUC in LDL_1 (upper panel) and LDL_2 (lower panel) in normolipidemic subject JT. Fraction numbers coincide with those given in Fig. 2 and are numbered from buoyant to dense. The symbols represent the observed data; the lines are drawn by hand. Each symbol represents a different LDL fraction (fx) as labeled.

creasing density. The initial rate of increase of radioactivity within fractions within the LDL_2 subpopulation occurred primarily in the more buoyant fractions. Radioactivity disappeared most rapidly from the more buoyant LDL_2 fractions (fx 17 and 18; $1.036 < d < 1.045$ g/ml) and then slowed considerably in the denser fractions 19 through 21 ($1.045 < d < 1.060$ g/ml; Fig. 5, LDL_2).

In FCHL subject HM, the initial increase in radioactivity was similar and rapid in fractions 9–13 ($1.027 < d < 1.042$ g/ml) within the LDL_1 subpopulation with the peak of radioactivity approximately 1.5 days after the injection of the radiolabeled lipoproteins (**Fig. 6**, LDL_1). There was a similar rapid rise in radioactivity within fraction 13 ($1.042 < d < 1.044$ g/ml) of the LDL_1 subpopulation but the peak occurred slightly later (2.5 days). The disapperance of radiolabeled particles from the LDL_1 subpopulation was faster in fractions 9 and 10 and slowed progressively in fractions 11–13. Within the LDL_2 subpopulation, the peak in radioactivity occurred 2–2.5 days after the injection of the iodinated VLDL + IDL (Fig. 6, LDL_2). In contrast to JT, however, the disappearance of radioactivity was very similar in all fractions within the LDL_2 subpopulation and was virtually identical to the rate of clearance of radioactivity from fraction 13 within the LDL_1 subpopulation.

DISCUSSION

The current studies were designed to examine the conversion of plasma precursors to the various LDL subpopulations unique to each individual using density gradient ultracentrifugation. Although various DGUC or flotation methods have been used to describe LDL heterogeneity in more detail, only recently have these methods been used to study the metabolic behavior of lipoproteins (6, 7, 16, 20, 27, 28). DGUC provides some advantages over sequential ultracentrifugation such as decreased ultracentrifugation time, the characterization of LDL density heterogeneity unique to each subject, and greater detail in describing the relationships between physical and kinetic variability as well as among precursors and various LDL products (16, 20). In the current studies, the general LDL density characteristics varied among the subjects with peak densities ranging from 1.033 g/ml to 1.048 g/ml. In addition, various LDL density subpopulations within an individual were evident in four out of five of the subjects (20).

Several important characteristics of apoB metabolism have been suggested from the studies presented here. First, it took several hours to days after the maximal conversion of precursor into LDL product for the precursor-derived particles to resemble plasma LDL (Fig. 1, JT and Fig. 2). Second, radiolabeled precursors contributed rapidly to a broad density range of LDL products

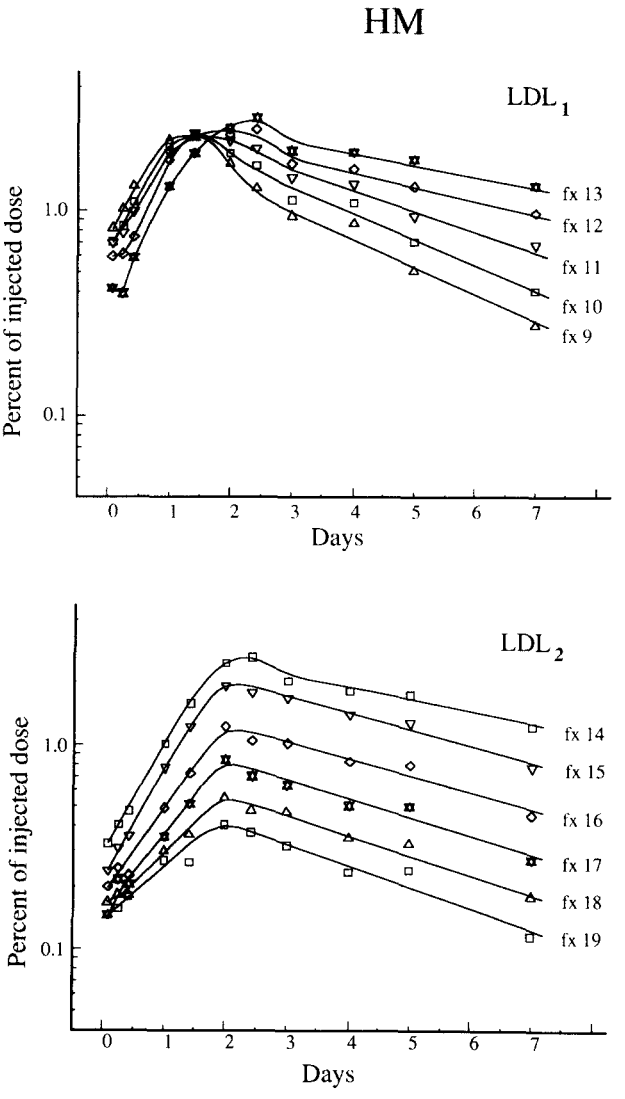

Fig. 6. The appearance and disappearance of VLDL + IDL-derived apoB radioactivity with time in each fraction isolated within the LDL density range after separation by DGUC in LDL_1 (upper panel) and LDL_2 (lower panel) in FCHL subject HM. Fraction numbers coincide with those given in Fig. 3 and are numbered from buoyant to dense. The symbols represent the observed data, the lines are drawn by hand. Each symbol represents a different LDL fraction (fx) as labeled.

(i.e., LDL_1 and LDL_2; Fig. 4); Third, in two out of the five subjects (HM and WE), the precursors did not contribute uniformly to all plasma LDL density subpopulations (Fig. 3). Fourth, with time the distribution of the precursor-derived LDL changed in relationship to the individual's plasma LDL protein mass in three out of five subjects (JT, MC, and DW; Fig. 2). And finally, the kinetic characteristics of particles within LDL appeared to change within a narrow density range and were not necessarily related to the physical density heterogeneity of each subject (Fig. 5, LDL_2; Fig. 6, LDL_1).

Traditionally, the relationship between VLDL precursors and LDL products has been described by following

the disappearance of radioactivity from VLDL ($d < 1.006$ g/ml) and its subsequent appearance in LDL ($1.019 < d < 1.063$ g/ml) using sequential ultracentrifugation (reviewed in 29). However, the data obtained using these conventional methods represents the sum of the radioactivity distributed among all the potential LDL products (subpopulations). For each subject in the current studies, the appearance of precursor-derived radioactivity as well as the distribution of these radiolabeled lipoproteins among LDL subpopulations was examined at each time point using DGUC. Using these techniques, the precursor-derived particles were more buoyant and non-superimposable with the LDL protein mass at the time point in which the maximum amount of precursor-derived radioactivity was isolated within the LDL density range defined uniquely for each subject (Fig. 1 vs Figs. 2 and 3). Although, by definition, all the radioactivity isolated within the LDL density range represents low density lipoproteins, these studies suggest that it takes up to several days for the precursor-derived particles to resemble the plasma LDL density characteristics unique to each subject. These observations may have important implications concerning the contribution of plasma precursors to various LDL products. That is, the contribution of VLDL and IDL to the major dense LDL subpopulation may be far less than predicted from the traditional plasma VLDL precursor-LDL product curves. Detailed quantitative analyses will help in understanding these relationships and are currently underway. It is of interest to note that the rate of conversion of VLDL-IDL precursors to LDL products was statistically correlated to total plasma cholesterol, VLDL cholesterol, plasma TG, and apoB concentrations, but not LDL cholesterol concentrations. In addition, no statistically significant correlations were found between these variables and the amount of radiolabeled precursor apoB that was converted to LDL apoB (data not shown). Although the biological significance of these observations is not known, it again reflects the complexity of apoB metabolism and the need to have a better understanding of the relationships between VLDL and LDL production.

Conceptually, it is thought that plasma LDL arises from the delipidation of VLDL to IDL and then to LDL, presumably, buoyant LDL to dense LDL. This conversion appears to involve several processes including intravascular enzymes such as lipoprotein lipase and hepatic lipase which hydrolyze the core triglycerides of the precursor particles and the loss of surface constituents (PL, FC, and apoproteins) which are transferred to high density lipoproteins (reviewed in 30). However, the results from the current studies suggest that plasma precursors contributed rapidly to a broad density range of LDL. As shown in Fig. 4, the initial appearance of precursor-derived radioactivity in LDL_1 and LDL_2 was approximately parallel. That is, the initial conversion of VLDL + IDL to buoyant ($1.026 < d < 1.036$ g/ml; density ranges for both subject's LDL_1 combined) and dense ($1.036 < d < 1.069$ g/ml; density ranges for both subjects' LDL_2 combined) LDL subpopulations was similar. Recently, Teng et al. (6) have shown the rapid conversion of radiolabeled plasma VLDL into visually separated 'light LDL' (mean density 1.0405 g/ml) and 'heavy LDL' (mean density 1.048 g/ml) in normolipidemic subjects, but not in familial hypercholesterolemic (FH) subjects. In addition, Huff and Telford (31) have published similar observations in miniature pigs. It is unclear whether specific LDL subpopulations are derived from certain precursors. For example, buoyant LDL subpopulations might be derived preferentially from specific precursors such as certain VLDL precursors, while the dense LDL subpopulations might be derived preferentially from IDL precursors. This could help explain the rapid conversion of precursors into buoyant as well as dense LDL subpopulations. This hypothesis and others can be tested using complex compartmental modeling; however, studies designed to test the preferential conversion of certain precursors to specific products will need to be done to address this possibility directly.

In two out of the five subjects (FCHL subjects WE and HM), the plasma precursors did not appear to contribute equivalently to all LDL subpopulations. At no time throughout the time course of each study was the distribution of the precursor-derived LDL superimposable with the distribution of the plasma LDL protein (Fig. 3, last panel). Although it is possible that, with additional time, the precursor-derived particles were metabolized to the dense LDL subpopulations, the overall contribution of the precursors to these LDL subpopulations would have been minimal. That is, less than 6% of the injected dose of precursor lipoprotein apoB remained in plasma at the end of these studies of which 2.8% and 1.7% (WE and HM, respectively) was isolated within the dense LDL_2 fraction. In the three normolipidemic subjects, in at least one point throughout each study, the distribution of the precursor-derived LDL resembled the distribution of the plasma LDL protein (Fig. 2, middle panel). These observations support the recent work of Teng et al. (6) in which the conversion of VLDL to IDL to buoyant LDL to dense LDL was seen in normolipidemic and hyperapobetalipoproteinemic subjects, but not in FH subjects. Although the limited number of study subjects presented here limits our ability to make general statements on the potential differences in the conversion of plasma precursors to specific LDL products between normolipidemic and FCHL subjects, it is interesting to speculate on the possibility that the small dense LDL characteristic of FCHL subjects may be derived from plasma VLDL-independent sources in at least a subset of these patients.

Additional metabolic heterogeneity within precursor-derived LDL was observed in the normolipidemic subjects. As described above, at one point in time the

distribution of the precursor-derived LDL resembled the distribution of the plasma LDL protein in the normolipidemic subjects (3 days for JT, 1 day for MC, and 2 days for DW). However, with time the distribution of the precursor-derived LDL changed compared to the steady-state distribution of the plasma LDL protein mass. In subject JT, the radiolabeled LDL increased in density with time (Fig. 2, lower panel) while in subjects MC and DW, the radiolabeled LDL isolated in a buoyant region of the LDL density range (data not shown). Changes with time in the distribution of radiolabeled 'light' and 'heavy' LDL ($1.025 < d < 1.040$ and $1.050 < d < 1.063$ g/ml, respectively) have been seen in preliminary studies done in mildly hypertriglyceridemic subjects by Beltz, Young, and Witztum (27). Similar observations have been made by Luc and Chapman (28) in guinea pig LDL. It is unclear what influences the metabolic behavior of these particles although their interactions with intravascular enzymes must be important. Very few studies have examined the substrate specificity of different LDL subpopulations to various plasma enzymes. In our lab, preliminary studies have suggested that, in some subjects, buoyant LDL subpopulations or metabolic pools within this region may be preferential acceptors for HDL-derived cholesteryl esters (C. A. Marzetta, T. J. Meyers, and J. J. Albers, unpublished results). Studies examining substrate specificity of the key lipoprotein intravascular enzymes will be important in our understanding of the metabolic heterogeneity within LDL.

In the current studies, it was not possible to obtain apoB specific activity for each fraction isolated within plasma LDL. That is, the percentage of the total radioactivity associated with apoB was determined for the pooled LDL_1 and LDL_2 subpopulations only. Then, the percentage of apoB radioactivity in LDL_1 was used to correct all the LDL_1 fractions to apoB radioactivity and, likewise, the percentage of apoB radioactivity found in LDL_2 was used to correct all the LDL_2 fractions. These calculations could potentially lead to slight variations in the apoB radioactivity curves since larger more buoyant LDL are more likely to contain more apoE than the smaller more dense LDL (4, 5). However, even if the apoB corrections are slightly under- or over-estimated for any given fraction, this would affect the overall magnitude of each curve rather than change the kinetic characteristic of the curve, assuming the apoprotein compositions stayed constant throughout each study.

Since LDL density and kinetic heterogeneity were characterized in detail in each subject, it was possible to examine potential relationships between the physical and metabolic characteristics. As illustrated in normolipidemic subject JT, distinct differences in the metabolic behavior of the individual fractions occurred within a narrow density range (Fig. 5; fractions 18 and 19). This observation was consistent with the increase in peak density with time in the precursor-derived LDL compared to the steady-state LDL protein mass (Fig. 2, last panel). These changes, however, could not be predicted based on the physical characteristics of this subject's plasma LDL which was relatively homogeneous compared to the other subjects. In FCHL subject HM, a noticeable lag in the maximum conversion of precursor-derived radioactivity into LDL was seen within a narrow density range (Fig. 6; peak conversion 1.5 to 2 days for fxs 9–12 vs 2.5 days for fx 13). This fraction corresponded to the inflection point between the 'shoulder' of the buoyant portion of the LDL DGUC profile (LDL_1) and the more dense major peak (LDL_2; Fig. 3). This relationship between discrete changes in the kinetic behavior of certain LDL fractions and changes in the distribution of the LDL protein mass was also seen in FCHL subject WE, but no obvious relationships were seen between the physical and kinetic heterogeneity of LDL in the other normolipidemic subjects DW and MC (data not shown). Unpredictable differences in the metabolic behavior of specific radiolabeled LDL density fractions and the various density subpopulations characterized by DGUC were also seen in these same subjects when injected with radiolabeled plasma LDL (20). Although changes in the chemical compositions of plasma LDL when subdivided into different density ranges appear to change gradually and linearly (2), subtle changes in the apoprotein composition could help account for changes in the kinetic behavior of specific LDL fractions. As shown previously by Gibson et al. (4), large buoyant LDL have more apoE associated with them than do smaller, more dense LDL. Since apoE is an important ligand for receptor recognition, it is possible that the presence of apoE in some of these LDL fractions would influence its metabolic fate. Ultimately, it will be very informative to be able to analyze the lipid and apoprotein composition of each fraction isolated within each subject's LDL.

In summary, the conversion of plasma VLDL and IDL into various LDL subpopulations was analyzed using density gradient ultracentrifugation in five subjects. The observations made using this approach suggested: *1*) it may take several days of intravascular processing of precursor-derived LDL to resemble the distribution of plasma LDL protein; *2*) VLDL and IDL precursors contributed rapidly to a broad density range of LDL products; *3*) the radiolabeled plasma precursors did not always contribute uniformly to all LDL subpopulations; *4*) with time, the distribution of the precursor-derived LDL changed in relationship to the distribution of the LDL protein mass in some subjects; and *5*) the kinetic characteristics of particles within LDL changed within a relatively narrow density range and were not always correlated to the density heterogeneity defined uniquely for each subject. It is clear from the current studies that LDL metabolism is very complex. Although density gradient ultracentrifugation is just one methodological tool

in which more detailed observations on the relationships between the physical and kinetic heterogeneity of LDL can be made, other methods such as gel filtration (16) and nondenaturing gradient gel electrophoresis (32). Combinations of these methods will help further our knowledge of the production and subsequent metabolism of various LDL subpopulations.

The authors would like to thank the Clinical Research Center staff; John Hokanson and Janet Adolphson for their technical expertise; and the study subjects for their cooperation. This work was supported by NIH grants HL-30086, RR-02176, and RR-36. C. A. M. was supported by an Institutional National Research Service Award (HL-07312).

Manuscript received 22 June 1989, in revised form 20 October 1989, and in re-revised form 26 January 1990.

REFERENCES

1. Fisher, W. R., M. F. Hammond, and G. L. Warmke. 1972. Measurements of the molecular weight variability of plasma low density lipoproteinemia. Demonstration of macromolecular-heterogeneity. *Biochemistry.* **11:** 519–525.
2. Shen, M. M. S., R. M. Krauss, F. T. Lindgren, and T. M. Forte. 1981. Heterogeneity of serum low density lipoproteins in normal subjects. *J. Lipid Res.* **22:** 236–244.
3. Krauss, R. M., and D. J. Burke. 1982. Identification of multiple subclasses of plasma low density lipoproteins in normal humans. *J. Lipid Res.* **23:** 97–104.
4. Gibson, J. C., A. Rubenstein, P. R. Bukberg, and W. V. Brown. 1983. Apolipoprotein E-enriched lipoprotein subclasses in normolipidemic subjects. *J. Lipid Res.* **24:** 886–898.
5. Lee, D. M., and P. Alaupovic. 1986. Apolipoprotein B, C-III, and E in two major subpopulations of low-density lipoproteins. *Biochim. Biophys. Acta.* **879:** 126–133.
6. Teng, B., A. D. Sniderman, A. K. Soutar, and G. R. Thompson. 1986. Metabolic basis of hyperapobetalipoproteinemia. Turnover of apolipoprotein B in low density lipoprotein and its precursors and subfractions compared with normal and familial hypercholesterolemia. *J. Clin. Invest.* **77:** 663–672.
7. Vega, G. L., and S. M. Grundy. 1986. Kinetic heterogeneity of low density lipoproteins in primary hypertriglyceridemia. *Arteriosclerosis.* **6:** 395–406.
8. Foster, D. M., A. Chait, J. J. Albers, R. A. Failor, C. Harris, and J. D. Brunzell. 1986. Evidence for kinetic heterogeneity among human low density lipoproteins. *Metabolism.* **35:** 685–696.
9. Berman, M., M. Hall, R. I. Levy, S. Eisenberg, D. W. Bilheimer, R. Phair, and H. Goebel. 1978. Metabolism of apoB and apoC lipoproteins in man: kinetic studies in normal and hyperlipoproteinemic subjects. *J. Lipid Res.* **19:** 38–56.
10. Zech, L. A., S. M. Grundy, D. Steinberg, and M. Berman. 1979. Kinetic model for production and metabolism of very low density lipoprotein triglycerides. Evidence for a slow production pathway and results for normolipidemic subjects. *J. Clin Invest.* **63:** 1262–1273.
11. Johnson, F. L., R. W. St. Clair, and L. L. Rudel. 1983. Studies on the production of low density lipoproteins by perfused livers from African green monkeys. Effects of dietary cholesterol. *J. Clin. Invest.* **72:** 221–235.
12. Johnson, F. L., R. W. St. Clair, and L. L. Rudel. 1985. Effects of the degree of saturation of dietary fat on the hepatic production of lipoproteins in the African green monkey. *J. Lipid Res.* **26:** 403–417.
13. Johnson, F. L., L. L. Swift, and L. L. Rudel. 1987. Nascent lipoproteins from recirculating and nonrecirculating liver perfusions and from the hepatic Golgi apparatus of African green monkeys. *J. Lipid Res.* **28:** 549–564.
14. Jones, L. A., T. Teramoto, D. J. Junh, R. B. Goldberg, A. H. Rubenstein, and G. S. Getz. 1984. Characterization of lipoprotein produced by the perfused rhesus monkey liver. *J. Lipid Res.* **25:** 319–335.
15. Teramoto, T., H. Kato, Y. Hashimoto, M. Kinoshita, T. Watanabe, H. Oka, and C. Naito. 1987. Effect of dietary cholesterol on production of lipoproteins and apolipoproteins by perfused livers from Japanese monkeys (*Macaca fuscata*). *Eur. J. Clin. Invest.* **17:** 522–529.
16. Marzetta, C. A., F. L. Johnson, L. A. Zech, D. M. Foster, and L. L. Rudel. 1989. Metabolic behavior of hepatic VLDL and plasma LDL apoB-100 in African green monkeys. *J. Lipid Res.* **30:** 357–370.
17. Beltz, W. F., Y. A. Kesaniemi, B. V. Howard, and S. M. Grundy. 1985. Development of an integrated model for analysis of the kinetics of apolipoprotein B in plasma very low density lipoproteins, intermediate density lipoproteins, and low density lipoproteins. *J. Clin. Invest.* **76:** 596–603.
18. Shephard, J., and C. J. Packard. 1987. Metabolic heterogeneity in very low-density lipoproteins. *Am. Heart J.* **113:** 503–508.
19. Fisher, W. R., L. A. Zech, P. Bardalye, G. Warmke, and M. Berman. 1980. Metabolism of apolipoprotein B in subjects with hypertriglyceridemia and polydisperse LDL. *J. Lipid Res.* **21:** 760–774.
20. Marzetta, C. A., D. M. Foster, and J. D. Brunzell. 1989. Relationships between LDL density and kinetic heterogeneity in subjects with normolipidemia and familial combined hyperlipidemia using density gradient ultracentrifugation. *J. Lipid Res.* **30:** 1307–1317.
21. McFarlane, A. S. 1958. Efficient-trace labeling of proteins with iodine. *Nature (London).* **182:** 53–57.
22. Bilheimer, D. W., S. Eisenberg, and R. I. Levy. 1972. The metabolism of very low density lipoprotein proteins. Preliminary in vitro and in vivo observations. *Biochim. Biophys. Acta.* **260:** 212–221.
23. Yamada, N., and R. J. Havel. 1986. Measurement of apolipoprotein B radioactivity in whole plasma by precipitation with isopropanol. *J. Lipid Res.* **27:** 910–912.
24. Marzetta, C. A., and L. L. Rudel. 1986. A species comparison of low density lipoprotein heterogeneity in nonhuman primates fed atherogenic diets. *J. Lipid Res.* **27:** 753–762.
25. Lipid Research Clinics Program. 1980. Manual of Laboratory Operations, Vol. I: Lipid and Lipoprotein Analysis. NIH, Publication # 80-1527.
26. Albers, J. J., V. G. Cabana, and W. R. Hazzard. 1975. Immuno-assay of human plasma apolipoprotein B. *Metabolism.* **24:** 1339–1351.
27. Beltz, W. F., S. G. Young, and J. L. Witztum. 1987. Heterogeneity in low density lipoprotein metabolism. *In* Proceedings of the Workshop on Lipoprotein Heterogeneity. K. Lippel, editor. NIH Publication #87-2646. 215–236.
28. Luc, G., and M. J. Chapman. 1988. Guinea pig low density lipoproteins: structural and metabolic heterogeneity. *J. Lipid Res.* **29:** 1251–1263.
29. Kesaniemi, Y. A., G. L. Vega, and S. M. Grundy. 1982. Kinetics of apolipoprotein B in normal and hyperlipidemic man.

Review of current data. *In* Lipoprotein Kinetics and Modeling. M. Berman, S. M. Grundy, and B. V. Howard, editors. Academic Press, San Francisco, CA. 181–205.
30. Gotto, A. M., H. J. Pownall, and R. J. Havel. 1986. Introduction to the plasma lipoproteins. *Methods Enzymol.* **128:** 3–41.
31. Huff, M. W., and D. E. Telford. 1989. Regulation of low density lipoprotein apoprotein B metabolism by lovastatin and cholestyramine in miniature pigs: effects on LDL composition and synthesis of LDL subfractions. *Metabolism.* **38:** 256–264.
32. Musliner, T. A., K. M. McVicker, J. F. Iosefa, and R. M. Krauss. 1987. Metabolism of human intermediate and very low density lipoprotein subfractions from normal and dyslipoproteinemic plasma. In vivo studies in the rat. *Arteriosclerosis.* **7:** 408–420.